DOI: 10.1002/chem.201001170

Effect of pH and Counterions on the Encapsulation Properties of Xenon in Water-Soluble Cryptophanes

Patrick Berthault,*[a] Hervé Desvaux,[a] Thierry Wendlinger,[a] Marina Gyejacquot,[a] Antoine Stopin,[b] Thierry Brotin,[b] Jean-Pierre Dutasta,[b] and Yves Boulard[c]

Abstract: In the ^{129}Xe NMR-based biosensing approach in which the hyperpolarized noble gas is transported to biological receptors for a sensitive molecular imaging, cryptophanes are excellent xenon host systems. However to avoid formation of self-organized systems, these hydrophobic cage molecules can be rendered water soluble by introduction of ionic groups. We show that the sensitivity of xenon to its local environment and the presence of these ionic functions can lead to interesting properties. For a first water-soluble cryptophane derivative, we show that a precise monitoring of the local pH can be performed. For a second cryptophane, the presence of ionic groups close to the cryptophane cavity modifies the xenon binding constant and in–out exchange rate. The latter allows the tuning of physical properties of xenon–cryptophane interactions without resorting to a change of the cavity size. These results open new perspectives on the influence of chemical modifications of cryptophanes for optimizing the biosensor properties.

Keywords: cryptophanes · hyperpolarization · NMR spectroscopy · sensors · xenon

Introduction

In 2001, the group of Pines introduced a molecular imaging approach combining the use of hyperpolarized ^{129}Xe and biosensors for high selectivity and high sensitivity magnetic resonance imaging (MRI).[1] The sensitivity is provided by the huge signal enhancement ($>10^4$) afforded by the optical pumping step, while the chemical sensitivity results from the strong dependence on the xenon chemical shift to its surroundings.[2] Since the weak[3] and non-specific[4] affinity of xenon to various proteins actually forbids its direct use as a probe of given biological receptors, the idea consisted of the encapsulation of the noble gas in hosts containing functional ligands that provided the biological specificity.

When caged, xenon possesses its own spectral signature (its own resonance frequency); a spectroscopic discrimination from free dissolved xenon is therefore allowed that opens access to localization of the receptors in a chemical shift imaging approach.[2] The sensitivity of xenon to its environment is so high that even a slight modification of the host can induce a chemical shift variation for caged xenon. Significant effects have been shown according to the diastereomery of the cage molecule,[5] its level of deuteration,[6,7] and even interaction of some remote tethered groups with their ligands.[1,8] Although this MRI–biosensing approach has for the moment never been applied in vivo, the proof-of-concept had been made on the avidin–biotin system,[9] and it was also successful for the detection of metalloproteinase activity,[10] of DNA strand hybridization,[8] or of proteins at the cellular surface.[11]

With a unique exception in which zeolite nanoparticles were used,[12] to date all ^{129}Xe NMR-based biosensors use cryptophane cores as xenon host molecules. They are nearly spherical cage molecules composed of two cyclotriveratrylene (CTV) bowls connected by three aliphatic linkers. The rigid bowl-shape structure of the cryptophane cavity generates a lipophilic cavity suitable for the encapsulation of xenon. According to their cavity volumes, their affinity to the noble gas, as well as the xenon in–out exchange rates

[a] Dr. P. Berthault, Dr. H. Desvaux, T. Wendlinger, M. Gyejacquot
IRAMIS, SIS2M, Laboratoire Structure et
Dynamique par Résonance Magnétique
UMR CEA/CNRS 3299, CEA-Saclay
91191 Gif-sur-Yvette (France)
Fax: (+33) 169089806
E-mail: patrick.berthault@cea.fr

[b] Dr. A. Stopin, Dr. T. Brotin, Dr. J.-P. Dutasta
Laboratoire de Chimie de l'ENS Lyon
UMR 5182 CNRS-ENS Lyon
Ecole Normale Supérieure de Lyon
46, Allée d'Italie, 69364 Lyon cedex 07 (France)

[c] Dr. Y. Boulard
IBITEC-S, Service de Biologie Intégrative et
Génétique Moléculaire, Laboratoire de Biologie Intégrative
CEA-Saclay, 91191 Gif-sur-Yvette (France)

vary.[13] A dedicated chemistry has been developed to further increase the xenon binding constants.[14] However, the hydrophobic character of these aromatic cage molecules can be problematic in the biosensing approach, since to obtain a water-soluble biosensor the insertion of a hydrophilic spacer is required.[15] The consequent amphiphilic character of such cryptophane-based biosensors can lead to the unwanted formation of self-organized molecular assemblies.[8] Therefore, part of the current chemical developments aims at rendering the cryptophane part itself more hydrophilic, for instance by substituting the methoxy groups of the original cryptophanes.

Herein, we show that the presence of ionizable groups on these new-generation cryptophanes leads to interesting spectral properties for caged xenon, giving rise to chemical sensors even in the absence of specific ligands. The interaction of laser-polarized xenon with two cryptophanes derived from cryptophane-A (i.e., in which the cyclotriveratrylene moieties are linked by ethylenedioxy groups) is studied. The first compound **1** has six carboxylic functions and has been used for assessing the concept of interleaved multiplexed MRI experiments based on ^{129}Xe biosensors.[16] In the present study, we show that this xenon host molecule constitutes a very sensitive probe of the local pH. The second water-soluble cryptophane **2**, which has six phenol functions, exhibits peculiar properties. Indeed, the influence of the nature of the counterion on both the xenon binding constant and the xenon in–out exchange is representative of what can be encountered when the ionizable groups of the cryptophane are close to the cavity.

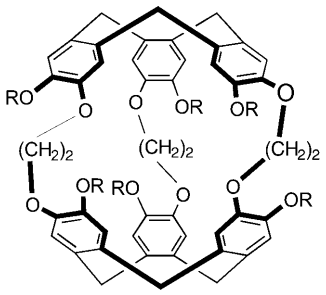

1: R = CH_2COOH **2**: R = H

Results and Discussion

pH Determination by using ^{129}Xe NMR spectroscopy: The ^{129}Xe NMR spectra of hyperpolarized xenon in an aqueous solution containing compound **1** show a peak at $\delta =$ 196 ppm, which is assigned to xenon free in water, and a peak in the region $\delta = 67$–73 ppm, corresponding to the noble gas encapsulated in **1**. In the high-field region, monitoring of the peak frequency of caged xenon reveals a variation in a range of about 3 ppm according to pH (Figure 1; inset). A plot of the chemical shift of caged xenon versus

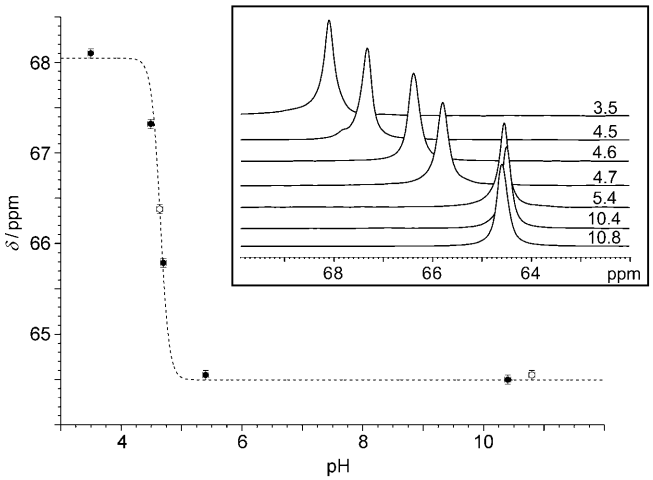

Figure 1. Plot of the chemical shift of xenon caged in **1** as a function of pH (data extracted from the spectra shown in the inset after deconvolution of the lines). The two white symbols correspond to experiments in which the pH was adjusted with KOD instead of NaOD. The best-fit theoretical curve to Equation (1) is superimposed (dashed line). Due to solubility reasons, it was not possible to acquire spectra at pH lower than 3.5.

$-\log(^2H^+)$ is reported in Figure 1. The data points follow a very pronounced sigmoidal curve. A fit to the function

$$\delta_{obs} = \delta_{base} - \frac{\Delta\delta}{1 + 10^{6(pH - pK_a)}} \quad (1)$$

(curve superimposed on Figure 1) provides the following values: $\delta_{base} = 64.55 \pm 0.1$ ppm ; $\Delta\delta = 3.55 \pm 0.17$ ppm. Taking into account the precision of the p^{2}H measurement, the extracted inflexion point value appears at 4.65 ± 0.05. According to reference [20], the correction due to the isotopic ^{1}H/^{2}H effect gives a value of 4.74 for pH, close to the pK_a of acetic acid (4.7). Attempting to fit the data points to several sigmoids does not significantly improve the agreement, tending to validate the assumption of six independent acidic functions for cryptophane **1**.

We have checked that the chemical shift of caged xenon does not depend on the solute concentration. Also, since the peaks always have almost the same linewidth (Figure 1; inset), the observed variation should not be an effect of the xenon in–out exchange rate. The ionic strength, different in each case, but with no correlation with the pH, does not also seem to play a role on the caged xenon chemical shift. Finally, the nature of the cation of the base appears of negligible impact since two points on this curve (Figure 1, white symbols) were obtained after adjusting the pH with KOD instead of NaOD.

The origin of the observed chemical shift variation as a function of pH can be rationalized by the variation induced by the presence or absence of anions on the aromatic rings bordering the cavity and by the change of the electronic density experienced by caged xenon, potentially resulting from the variation of the cation density.[21] In any case, the present result indicates that using compound **1** the chemical

shift of caged xenon can be highly sensitive to the pH in the region close to the pK_a opening interesting perspectives in terms of in vivo applications. Indeed, whereas in ^{31}P NMR spectra the signals are shifted by a maximum of 2.5 ppm for 5 pH units for inorganic phosphate,[22] here a variation of 3 ppm is observed per pH unit in the pK_a region. Moreover, the high mobility of the noble gas that leads to narrower lines than in ^{31}P NMR spectra combined with the sensitivity improvement allowed by hyperpolarization should facilitate such in vivo experiments.

Finally, with respect to the recent work of Gosset et al.,[23] in which aminophosphonate molecules were used as pH probes by ^{31}P NMR spectroscopy, the greatest interest of the xenon approach resides in the much lower concentration range (μM instead of mM) offered by the optical pumping state.

Influence of the counterion on the xenon binding

Structural effect: Cryptophane **2**, which has six phenol functions, is soluble (mM range) in basic conditions. Compared with all previously used water-soluble cryptophanes, the ionizable groups of compound **2** are now much closer to the cavity entrances. For this system, the very low solubility at neutral pH preventing its detection by ^{1}H NMR spectroscopy forbids accurate monitoring of the caged ^{129}Xe chemical shift as a function of the pH. In the basic range this chemical shift appears very weakly dependent on the pH, but strongly dependent on the nature of the counterion, illustrating the existence of competitive equilibria.

Figure 2 displays the ^{129}Xe NMR spectra obtained at pH 12.2 using four different bases (LiOD, NaOD, KOD, and CsOD) to adjust the pH with the same amount of xenon and the same cryptophane **2** concentration. The first striking observation is that with Cs^+, only one peak appears on the ^{129}Xe spectrum. It corresponds to the chemical shift of xenon in water; the peak featuring Xe@**2** in the $\delta = 60$–70 ppm range is absent. Given that several experiments with various cage concentrations did not reveal any chemical shift variations indicative of a fast exchange on the ^{129}Xe chemical shift time scale, this suggests that xenon does not enter in the cryptophane cavity for this solution.

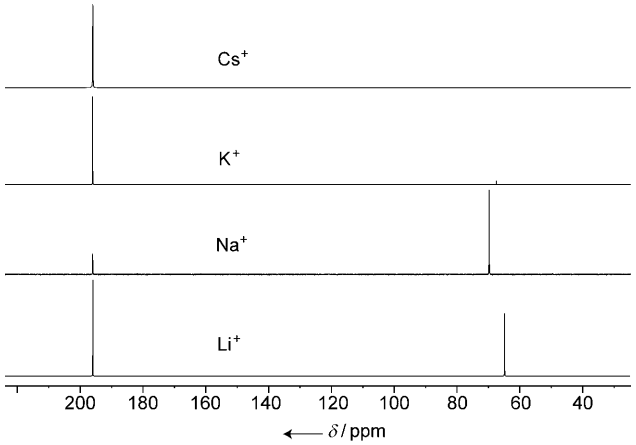

Figure 2. ^{129}Xe NMR spectra of solutions containing compound **2** at 293 K. The bases used to adjust the pH to 12.2 were CsOD, KOD, NaOD, and LiOD, from top to bottom. No signal in the $\delta = 60$–70 ppm range can be detected in the case of the Cs ion.

For the three other cations, two peaks appear on the ^{129}Xe spectrum, with different intensity ratios giving an estimation of the noble gas binding constants to the cage in these environments. Typically, we are facing competition between cation–cryptophane and xenon–cryptophane equilibria. The variation of the Xe@**2** chemical shift according to the nature of the counterion indicates a different electronic density around the caged noble gas and/or a different cryptophane conformation. These two mechanisms were already invoked for explaining a modification of vibrational circular dichroism spectra[17] or chemical shift variations under xenon binding.[24]

From the ^{1}H NMR spectra of **2** in the degassed solutions (not shown), whatever the counterion, two remarks can be made. Firstly, the degassed spectrum exhibits slightly sharper lines than the spectrum obtained just after dissolution of the cryptophane. Removal of the oxygen encapsulated in the cavity should be responsible for this effect. Secondly, whereas compound **1** has been shown to exist in aqueous solution in two forms in very slow exchange, that is, crown–crown and crown–saddle in which one of the methylene protons of the cyclotriveratrylene (CTV) is oriented towards the center of the cavity and not to its exterior,[7] no such situation occurs for compound **2**. For instance, the aromatic region contains only two peaks corresponding to protons in the *ortho*- and *meta*-positions from the phenol group resulting either from a symmetrical molecule or from fast conformational exchange. Moreover, the whole observed chemical shifts correspond to a crown–crown configuration. The crown–crown/crown–saddle equilibrium is in fact never observed for this cryptophane whatever the counterion and the pH.

As displayed in Figure 3 the ^{1}H NMR spectra of the four solutions in the presence of the same amount of dissolved xenon reveal the influence of the counterion on the xenon binding process. Notably, after the introduction of xenon into solution, the lines of the ^{1}H NMR spectrum of **2** remain sharp. The first striking evidence is that the ^{1}H NMR spectrum of the sample containing Cs^+ ions is not modified by addition of xenon to the solution, confirming the absence of xenon binding observed in the ^{129}Xe NMR spectrum. The ^{1}H NMR spectrum of **2** in the Cs^+ solution displays only two well-resolved doublets in the aromatic region and for the aliphatic region, two doublets corresponding to the axial and equatorial protons of the cyclotriveratrylene, and two doublets in strong coupling conditions for the ethyleneoxide protons (protons of the linker OCH_2–CH_2O). For the samples containing K^+, Na^+, and Li^+, slow exchange conditions on the proton chemical shift timescale are observed (Figure 3). In the aromatic region, this results in a net splitting of the two peaks for the sample containing K^+ ions (the tiny peaks corresponding to the form filled with xenon) and

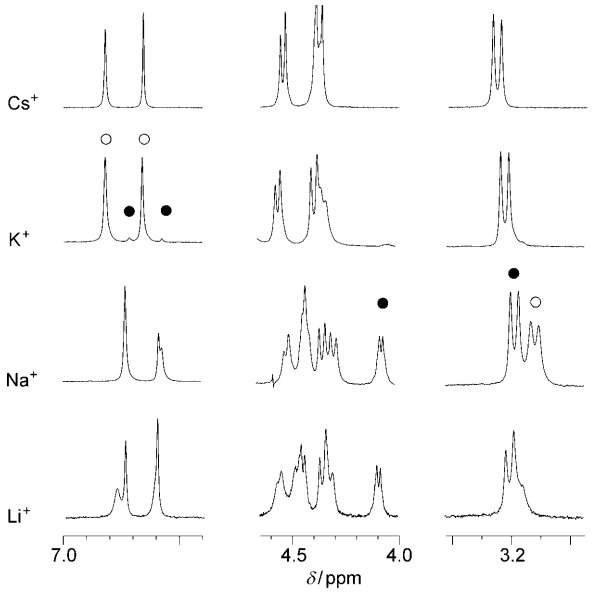

Figure 3. ^{1}H NMR spectra of solutions containing compound **2** at 293 K in the presence of dissolved xenon. The bases used to adjust the pH to 12.2 were CsOD, KOD, NaOD, and LiOD, from top to bottom. Only the spectral regions containing peaks are displayed, that is, the regions $\delta =$ 7.0–6.4 (left), 4.7–4.0 (middle), and 3.4–2.9 ppm (right). Symbols ● and ○ on some peaks of the K^+ and Na^+ solutions indicate the form filled with xenon and the empty form, respectively.

in smaller effects (peak shoulders) for Na^+ and Li^+. Note, however, that the main resonances of the aromatic protons are high field shifted for Na^+ and Li^+ with respect to Cs^+ and K^+.

Modifications of the ^{1}H NMR spectra in the region 4.7–4.0 ppm due to the slow exchange effect are much more pronounced for Na^+ and Li^+ than for K^+. This region corresponds to the (O-CH_2-CH_2-O) linker protons and the axial proton of the CTV part. An assumption, which is consistent with the observations of Luhmer et al.[24] and Bouchet et al.[17] is that this slow exchange dealing with the ethylenedioxy protons is due to the *trans*/*gauche* conformational change of the O-CH_2-CH_2-O torsion angle.

Finally, in the case of Na^+, striking changes in the high-field region corresponding to the equatorial proton of the CTV part, are also observed (splitting of the resonance). Surprisingly, the ^{1}H NMR spectrum signal corresponding to the empty form resonates at even higher field (checked with various amounts of xenon introduced in solution). This observation tends to indicate that the local structure of CTV is altered by the interactions between free cryptophane and sodium ions.

We can consequently safely conclude from these observations that in the presence of Cs^+, xenon does not enter into the **2** cavity. This is in agreement with the results obtained by vibrational circular dichroism.[17] Another conclusion is that the other cations strongly affect the xenon binding to compound **2**. A priori, two types of interactions between cations and **2** can be figured out. Either ions are able to occupy the cryptophane cavity, or their electrostatic interactions with the phenate groups slow down or even block the access to the hydrophobic cryptophane cavity. The observation of slow exchange conditions on the proton NMR time scale when the bulky DBU base (1,8-diazabicyclo-[5.4.0]undec-7-ene) is used for tuning the pH to 12.2 tends to privilege the second assumption. Also this assumption was put forward for explaining vibrational circular dichroism spectra in the presence of small neutral molecules.[17] Finally, this assumption is reinforced by the ionic radius of Cs^+ (1.67 Å) larger than that of the other alkali metals (K^+ $r_{ionic} = 1.33$ Å; Na^+ $r_{ionic} = 0.97$ Å; Li^+ $r_{ionic} = 0.68$ Å) which, as shown by DFT calculations of a free molecule, can more efficiently block the entrance[17] or could allow its stronger binding by the phenate groups, thus forbidding xenon complexation. Other spectroscopic arguments substantiate this interpretation: 1) The strong variation of the Xe@**2** chemical shift as a function of the counterion already evidences a change in the cryptophane structure and electronic density and 2) The observation of slow exchange conditions for either aromatic or aliphatic or axial protons of the CTV according to the cation used illustrates a change in the chemical equilibria between the different conformers in particular for the cryptophane linkers.

All these arguments do not allow the design of an experimentally validated structural and dynamical model of the complex, which could explain the origin of the strong interaction between cryptophane **2** and cations. Indeed, all attempts to directly characterize, for instance, the strong Cs^+–**2** interaction by dipolar polarization transfer (HOESY experiments[25]) or by triple-quantum filter experiments[26] were unsuccessful.

Xenon binding constant: The slow exchange conditions in the proton and xenon spectra are favorable to quantitative characterization of the xenon binding constant, since accurate knowledge of the xenon concentration can be avoided, although its determination is usually problematic due to the transient feature of hyperpolarized experiments and the dependence of xenon solubility on ions and pH. It remains that the structure of the complex involving cations and cryptophanes is presently ill defined, which prevents straightforward quantitative exploitations. As a consequence we only consider two simple models.

In the first one, the apparent (counterion-dependent) binding constants of xenon to compound **2** are derived. These values are the relevant one for biosensing application. In a second step, we compare the affinity of xenon to cryptophane **2** as a function of the used cation.

If [X], [C], $[C]_t$, and [XC] denote the concentrations of free xenon, of Xe-free cryptophane, of total cryptophane and of the Xe@**2** complex, respectively, the ratio measured between the two resonance peaks on the ^{129}Xe NMR spectrum is $f_{Xe} = [XC]/[X]$ and the relative integration of a peak corresponding to the empty cage and of another peak corresponding to the filled cage on the ^{1}H NMR spectrum gives: $f_H = [XC]/[C]$. Thus the apparent binding constant K_{app} can directly be obtained:

$$K_{app} = \frac{[XC]}{[X][C]} = \frac{f_{Xe}}{[C]} = \frac{f_{Xe}(1+f_H)}{[C]_t} \quad (2)$$

In Table 1 the apparent binding constant values are reported. Their analysis confirms the first tendency observed on the ^{129}Xe NMR spectra (Figure 2). For the range of ion concentrations used, the value of the xenon–cryptophane apparent binding constant is the largest for Na^+. However, these values are dependent on the presence and concentration of the counterion (I) since the latter acts as a competitor. The lack of knowledge on the cryptophane–ion interaction encouraged us to consider the simplest competitive equilibrium in which we neglect the existence of cryptophane free from both xenon and counterion, since its concentration is too low to be detected by ^{1}H NMR spectroscopy:

Table 1. Binding constants for xenon to cryptophane **2** corresponding to the two models as extracted from signal integration of the 11.7 T ^{129}Xe and ^{1}H NMR spectra acquired at 293 K.

Counterion	K_{app} [M^{-1}]	K
K^+	327 ± 15	6 ± 1
Na^+	1790 ± 90	20 ± 2
Li^+	475 ± 24	40 ± 4

$$X + IC \rightleftharpoons XC + I \quad (3)$$

In fact, according to the pH (>12) and the cryptophane concentration (about 1 mM) used, it seems reasonable to consider the following relations between the ion-dependent concentrations: $[I] \approx [I]_t \gg [IC]$. The constant K associated to this equilibrium is equal to:

$$K = \frac{[XC][I]}{[IC][X]} \approx K_{app}[I]_t \quad (4)$$

The deduced values are reported in Table 1. Typically the xenon binding constant K taking into account the embedding due to the counterion is 2 times larger for Li^+ than for Na^+ which is 4 times larger than for K^+. The tendency is in complete agreement with the above-reported structural interpretation, since the larger the ion radius, the bigger its affinity to the cryptophane. The size of the counterion is therefore a key parameter, as noticed recently using circular dichroism methods in reference [17].

Xenon in–out exchange rate: As clearly observed in the NMR spectra, for cryptophane **2** the nature of the cation present in solution influences both the apparent xenon binding constant and the xenon in–out exchange rate, the latter being now slow at the proton chemical shift time scale (i.e., in the Hz range). These observations are strikingly different to the case of compound **1** or other cryptophane-A derivatives,[13] which always are in fast exchange conditions on the proton chemical shift time scale, revealing exchange rates at least one order of magnitude faster (for instance its value is 100 Hz for compound **1**). A series of ^{1}H-EXSY experiments performed on the solutions of compound **2** in the presence of the noble gas and different counterions have allowed exchange characterization through the monitoring of the volume of one or several cross-peaks assigned to pure exchange with the mixing time. The in–out exchange rates at 293 K vary from 0.4 to 10 Hz. First of all, the comparison of these exchange rate values to the xenon longitudinal self-relaxation rate ($T1 \approx 8$ s) clearly indicates that hyperpolarized xenon spectra can be used for extracting thermodynamical parameters, such as binding constants. The in–out exchange rate follows the expected behavior along the ion series: for instance, it is two orders of magnitude faster in the case of Li^+ than for K^+.

This result is in complete agreement with the interpretation of the ions blocking the portals of the cryptophane cavity. Also, the temperature dependence of these exchange rates follows the expected behavior with an increase by a factor about 10 in the range 280–310 K. As previously noted, the inability to directly characterize the cation–cryptophane interactions renders fully quantitative exchange studies of limited interest, since we are facing competitive equilibria. Thus, it could either be the xenon entrance or exit or the ion exchange, which would be the limiting phenomenon. Nevertheless, considering the ^{129}Xe NMR spectroscopy based biosensing approach, the fact that the xenon exchange rate can so strongly be affected by the chemical structure of the cryptophane and the nature of counterion provides clues for optimizing the in–out exchange rate. The latter is indeed of key importance for biosensing experiments, since its value strongly influences the sensitivity enhancement allowed by exchange in direct detection[7,27] or by a HYPERCEST[9] (hyperpolarized xenon chemical-exchange saturation transfer) approach.

Conclusion

The present study provides new clues for the development of ^{129}Xe NMR spectroscopy based biosensors soluble in water that could be termed smart or activatable. In the same vein as temperature gating through xenon in–out exchange described by Schröder et al.,[28] we show here that addition of ionizable groups to the cryptophane core can lead to sensors of external conditions, such as local pH or the presence of given cations by means of NMR spectroscopy of hyperpolarized xenon.

Firstly, the study of cryptophane **1** illustrates that the development of cryptophanes with specific biological ligands is not necessarily required to obtain powerful biosensors. Indeed, by simply designing cryptophanes that have functional groups sensitive to the physical properties of the surrounding media (here pH) new promising probes are obtained. Since in addition it is known that cryptophane cell uptake can easily be achieved (through grafting of cell pene-

trating peptides for instance[29]), the internal chemical properties of cells could be probed. As an example such a modified cryptophane **1** would allow the location of cells of low pH (cells entering in acidose) since it already constitutes an interesting xenon host for the ^{129}Xe NMR spectroscopy based biosensing approach, allowing local pH measurement around 4.7. To probe more realistic biological pH, the synthesis of new cryptophanes containing groups with pK_a values in the region of 6–7 (such as imidazoles for instance) is underway in our laboratories.

Secondly, the study of a second cryptophane **2** reveals that modifications on the cage designed to increase its solubility in water can lead to unexpected embarrassing behavior, such as the inhibition of xenon binding (in the case of Cs^+ counterions). Also, this study reveals that the xenon in–out exchange rate can strongly be affected by the nature of the substituents on the cyclotriveratrylene part and the ions present. Finding routes to tune this exchange rate without resorting to the cage size is in fact a promising alternative solution since sensitive biosensing MRI requires narrow lines, that is, long apparent T_2 and thus a relatively slow exchange rate,[2] whereas multiplexing experiments require the use of different cryptophanes,[16] typically of different sizes, for which exchange rates can be not as ideal as cryptophane-A or cryptophane-111.

Experimental Section

Chemicals: The syntheses of compounds **1** and **2** have been described in references [17 and 18], respectively. Solutions of compounds **1** or **2** (1 mM in D_2O) were used. The pH was adjusted by addition of strong acids or bases, and measured on a dedicated pH meter. For the experimental results reported here, whatever the pH, the prepared NMR tube was perfectly limpid before and after addition of xenon. Xenon enriched at 86% in isotope 129 from Cortecnet was used throughout this study.

Preparation of laser-polarized xenon and NMR spectroscopy experiments: Xenon polarized at a level of 20–40% (signal enhancement 2.10^4 to 4.10^4) was produced in the batch mode by using our home-built apparatus described in references [2 and 19]. It was transported from the optical pumping site to the NMR spectrometer inside a solenoid producing a magnetic field of 3 kG immersed in liquid nitrogen. In the fringe field of the NMR magnet xenon is sublimated and transferred by cryo-condensation to the previously degassed NMR spectroscopy tube of interest by using a vacuum line. The amount of xenon introduced was checked after the experiment by weighting the tube before and after its degassing from the added xenon. All NMR experiments were performed on a Bruker Avance II 500 MHz spectrometer equipped either with direct (^{129}Xe/^{1}H) or inverse HTX probeheads. Except when mentioned, the temperature was 293 K. The free xenon signal in water was calibrated at 196 ppm. We have checked in the pH range 1.7–11.2 that (in the absence of cryptophane) the chemical shift of xenon dissolved in water varies by less than 1 ppm (calibration with respect to the xenon gas signal at 1 bar).

Acknowledgements

Support from the French Ministry of Research (projects ANR-06-PCVI-0023 BULPOXI and NT09-472096 GHOST) is acknowledged.

[1] M. M. Spence, S. M. Rubin, I. E. Dimitrov, E. J. Ruiz, D. E. Wemmer, A. Pines, S. Qin Yao, F. Tian, P. G. Schultz, *Proc. Natl. Acad. Sci. USA* **2001**, *98*, 10654–10657.
[2] P. Berthault, G. Huber, H. Desvaux, *Prog. Nucl. Magn. Reson. Spectrosc.* **2009**, *55*, 35–60.
[3] L. Dubois, P. Da Silva, C. Landon, J. G. Huber, M. Ponchet, F. Vovelle, P. Berthault, H. Desvaux, *J. Am. Chem. Soc.* **2004**, *126*, 15738.
[4] S. M. Rubin, S.-Y. Lee, E. J. Ruiz, A. Pines, D. E. Wemmer, *J. Mol. Biol.* **2002**, *322*, 425–440.
[5] J. G. Huber, L. Dubois, H. Desvaux, J.-P. Dutasta, T. Brotin, P. Berthault, *J. Phys. Chem. A* **2004**, *108*, 9608–9615.
[6] T. Brotin, A. Lesage, L. Emsley, A. Collet, *J. Am. Chem. Soc.* **2000**, *122*, 1171–1174.
[7] G. Huber, T. Brotin, L. Dubois, H. Desvaux, J.-P. Dutasta, P. Berthault, *J. Am. Chem. Soc.* **2006**, *128*, 6239–6246.
[8] V. Roy, T. Brotin, J.-P. Dutasta, M.-H. Charles, T. Delair, F. Mallet, G. Huber, H. Desvaux, Y. Boulard, P. Berthault, *ChemPhysChem* **2007**, *8*, 2082–2085.
[9] L. Schröder, T. J. Lowery, C. Hilty, D. E. Wemmer, A. Pines, *Science* **2006**, *314*, 446–449.
[10] Q. Wei, G. K. Seward, P. A. Hill, B. Patton, I. E. Dimitrov, N. N. Kuzma, I. J. Dmochowski, *J. Am. Chem. Soc.* **2006**, *128*, 13274–13283.
[11] A. Schlundt, W. Kilian, M. Beyermann, J. Sticht, S. Günther, S. Höpner, K. Falk, O. Roetzschke, L. Mitschang, C. Freund, *Angew. Chem.* **2009**, *121*, 4206–4209; *Angew. Chem. Int. Ed.* **2009**, *48*, 4142–4145.
[12] F. Lerouge, O. Melnyk, J.-O. Durand, L. Raehm, P. Berthault, G. Huber, H. Desvaux, A. Constantinesco, P. Choquet, J. Detour, M. Smaïhi, *J. Mater. Chem.* **2009**, *19*, 379–386.
[13] G. Huber, L. Beguin, H. Desvaux, T. Brotin, J.-P. Dutasta, P. Berthault, *J. Phys. Chem. A* **2008**, *112*, 11363–11372.
[14] T. Brotin, J.-P. Dutasta, *Chem. Rev.* **2009**, *109*, 88–130.
[15] T. J. Lowery, S. Garcia, L. Chavez, J. E. Ruiz, T. Wu, T. Brotin, J.-P. Dutasta, D. S. King, P. G. Schultz, A. Pines, D. E. Wemmer, *ChemBioChem* **2006**, *7*, 65–73.
[16] P. Berthault, A. Bogaert-Buchmann, H. Desvaux, G. Huber, Y. Boulard, *J. Am. Chem. Soc.* **2008**, *130*, 16456–16457.
[17] A. Bouchet, T. Brotin, D. Cavagnat, T. Buffeteau, *Chem. Eur. J.* **2010**, *16*, 4507–4518.
[18] L. Garel, B. Lozach, J.-P. Dutasta, A. Collet, *J. Am. Chem. Soc.* **1993**, *115*, 11652–11653.
[19] H. Desvaux, T. Gautier, G. Le Goff, M. Pétro, P. Berthault, *Eur. Phys. J. D* **2000**, *12*, 289–296.
[20] A. Krezel, W. Bal, *J. Inorg. Biochem.* **2004**, *98*, 161–166.
[21] C. Jameson, *Prog. Nucl. Magn. Reson. Spectrosc.* **1991**, *23*, 1375–1395.
[22] P. B. Garlick, G. K. Radda, P. J. Seely, *Biochem. J.* **1979**, *184*, 547–551.
[23] G. Gosset, S. Martel, J.-L. Clément, B. Blaive, G. Olive, M. Culcasi, R. Rosas, A. Thévand, S. Pietri, *C. R. Chim.* **2008**, *11*, 541–552.
[24] M. Luhmer, B. M. Goodson, Y. Q. Song, D. D. Laws, L. Kaiser, M. C. Cyrier, A. Pines, *J. Am. Chem. Soc.* **1999**, *121*, 3502–3512.
[25] C. Yu, G. Levy, *J. Am. Chem. Soc.* **1984**, *106*, 6533–6537.
[26] G. Jaccard, S. Wimperis, G. Bodenhausen, *J. Chem. Phys.* **1986**, *85*, 6282–6293.
[27] M. Spence, J. E. Ruiz, S. Rubin, T. J. Lowery, N. Winssinger, P. G. Schultz, D. E. Wemmer, A. Pines, *J. Am. Chem. Soc.* **2004**, *126*, 15287–15294.
[28] L. Schröder, L. Chavez, T. Meldrum, M. Smith, T. J. Lowery, D. E. Wemmer, A. Pines, *Angew. Chem.* **2008**, *120*, 4388; *Angew. Chem. Int. Ed.* **2008**, *47*, 4316.
[29] G. K. Seward, Q. Wei, I. J. Dmochowski, *Bioconjugate Chem.* **2008**, *19*, 2129–2135.

Received: May 1, 2010
Published online: September 30, 2010

